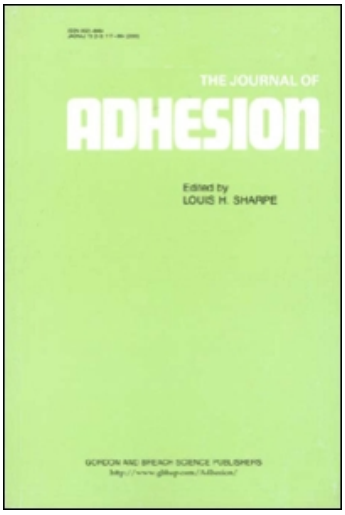

The Journal of Adhesion

Publication details, including instructions for authors and subscription information:
http://www.informaworld.com/smpp/title~content=t713453635

Strength Predictions for Lap Joints, Especially with Composite Adherends. A Review

Robert D. Adams[a]
[a] Department of Mechanical Engineering, University of Bristol, Bristol, England

To cite this Article Adams, Robert D.(1989) 'Strength Predictions for Lap Joints, Especially with Composite Adherends. A Review', The Journal of Adhesion, 30: 1, 219 — 242
To link to this Article: DOI: 10.1080/00218468908048207
URL: http://dx.doi.org/10.1080/00218468908048207

J. Adhesion, 1989, Vol. 30, pp. 219–242
Reprints available directly from the publisher
Photocopying permitted by license only

Printed in the United Kingdom

Strength Predictions for Lap Joints, Especially with Composite Adherends. A Review*

ROBERT D. ADAMS

Department of Mechanical Engineering, University of Bristol, Bristol BS8 1TR, England

(Received October 21, 1988; in final form June 12, 1989)

Classical linear solutions (such as Volkersen, Goland and Reissner) of the lap joint problem are discussed, together with more advanced versions of the same type. Finite element techniques are shown to be the best way of treating the non-linear mechanics and material behaviour in real joints. Finally, when applied to composite adherends, the principles given here show how the strength can be increased by up to 500%.

KEY WORDS Strength predictions; composite materials; finite element analysis; non-linear adhesive properties; local stress effects; improved strength.

1 INTRODUCTION

The design of engineering structures depends on knowing the loads and stresses which are likely to occur in practice. The loads are usually determined by the function of the structure and the engineer uses the best available materials and design techniques to arrive at a suitable and cost-effective solution. Recent advances in technology together with new and more demanding environments have resulted in a strong emphasis being placed in modern engineering on the need to quantify the structural loads and critical stresses. Not only are cost-effective products required, but consumer-oriented legislation seeks to blame the designer who was careless and allowed his structure to fail.

Design requires the ability to analyse. In bonded joints, analysis means determining the stresses and strains under given load conditions, so that predictions can be made of the likely points of failure. These predictions can be used with observations of actual fracture paths, to give a designer a qualitative and a quantitative understanding of the mechanics of adhesively-bonded joints.[1]

Some of the many different forms of structural lap joints are shown in Figure 1.

* Presented at the 35th Sagamore Army Materials Research Conference, Manchester, New Hampshire, U.S.A., June 26–30, 1988.

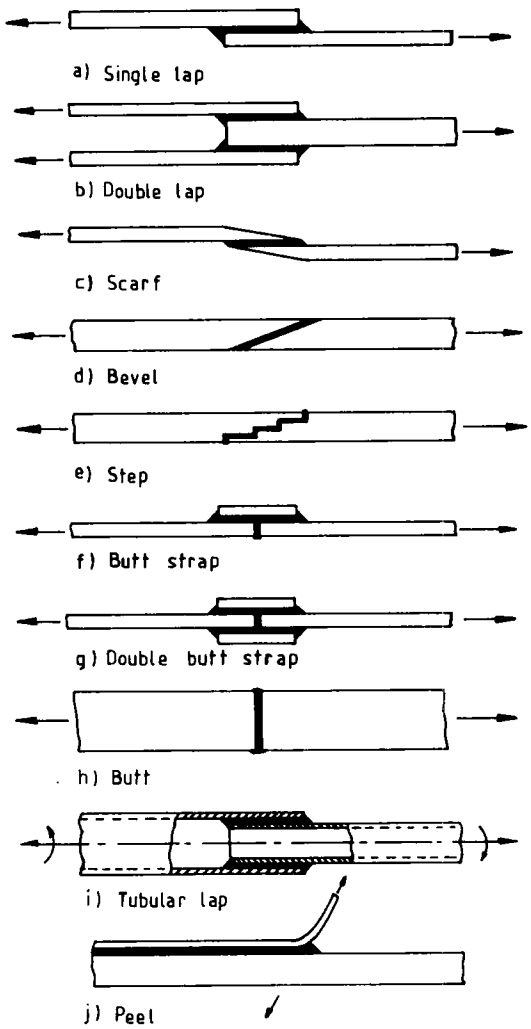

FIGURE 1 Some common engineering adhesive joints.

More complex joints exist, but first we need to understand the mechanics of the so-called "simple" joints.

Design follows analysis and understanding. It is based on the assumption that failure takes place in the adhesive (called cohesive failure) rather than between the adhesive and the adherend or substrate (called adhesive failure). The objective of this paper is to provide a critical assessment of the various theories and techniques used in analysing lap joints. Closed form analytical (algebraic) techniques are described, together with their disadvantages. It is then shown how finite element techniques can account for non-linear mechanics and materials, together with realistic adhesive bond-line geometries. When suitable failure criteria are used (obtained from bulk adhesive specimens), finite element

techniques can predict accurately the joint strength from first principles, knowing only the geometry, loading, and material properties. Finally, the technique is applied to bonded joints using adherends made from composite materials such as fibre reinforced plastics and it will be shown how a fivefold increase in the strength of lap joints was both predicted theoretically and confirmed experimentally.

2 CLASSICAL LINEAR, ELASTIC SOLUTIONS

The average shear stress τ for a simple lap joint is given by

$$\tau = P/bl$$

where P is the applied load, b is the joint width, and l is the joint length as shown in Figure 2(a). This simple equation is as far as many designers go when analysing stresses, and it is the definition of adhesive shear strength used in standard tests such as ASTM D 1002-72. This is, of course, rather simplistic and takes no account of the flexibility of the adhesive and the adherends.

Volkersen[2] tried to analyse the stresses in rivetted panels, but could only deal with the case of an infinite number of tiny rivets, which effectively created a continuum, for which he developed his well-known shear-lag equations. The continuum is, of course, identical to the case of an adhesive layer. Volkersen assumed that the adhesive deformed only in shear and the adherends deformed

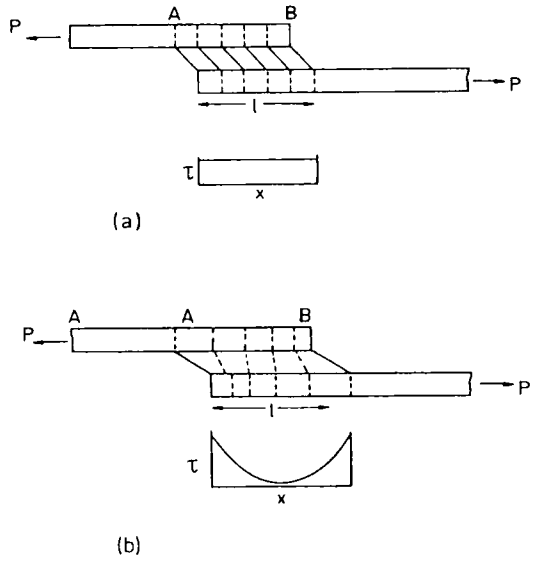

FIGURE 2 Exaggerated deformations in loaded single lap joint:
(a) with rigid adherends;
(b) with elastic adherends.

only in tension. The equations are well-known and give the shear stress distribution shown in Figure 2(b), which should be compared with the constant distribution of shear stress given in Figure 2(a) which is the case when the adherends are considered to be rigid. In practice, the adherend tensile stress decreases progressively from a maximum at the loaded end to zero at the unloaded end. The rate of change of adherend stress depends mainly on the stiffness of the adherends, as shown by Volkersen's equations. The stresses in the adjacent adherends will be a mirror image of this for equal adherends, as is shown scehmatically in Figure 2(b). The shear strain (and stress) in the adhesive layer is a maximum at each end, and a minimum in the middle. If the adherends are not of equal stiffness, the adhesive shear and adherend tensile stresses will be asymmetric.

Volkersen neglected several important factors. First, because the directions of the two forces in Figure 2 are not collinear, there must be a bending moment applied to the joint in addition to the in-plane tension. The adherends bend and the rotation alters the direction of the load line in the region of the overlap to form a geometrically non-linear problem. Thus, the joint displacements are no longer directly proportional to the applied load. Goland and Reissner[3] took this effect into account by using a bending moment factor, k, which relates the bending moment on the adherend at the end of the overlap, M_0, to the in-plane loading, by the relationship,

$$M_0 = kPt/2$$

where t is the adherend thickness (the thickness of the adhesive layer was neglected), (see Figure 3). If the load on the joint is very small, no rotation of the overlap takes place, so $M_0 = Pt/2$ and $k = 1.0$. As the load is increased, the overlap rotates, bringing the line of action of the load closer to the centre-line of the adherends, thus reducing the value of the bending moment factor. Goland and Reissner give a similar shear stress distribution to that of Volkersen, but also give the transverse tearing (peel) stresses in the adhesive layer as shown in Figure 4. The shear and peel stresses were both assumed to be uniform across the

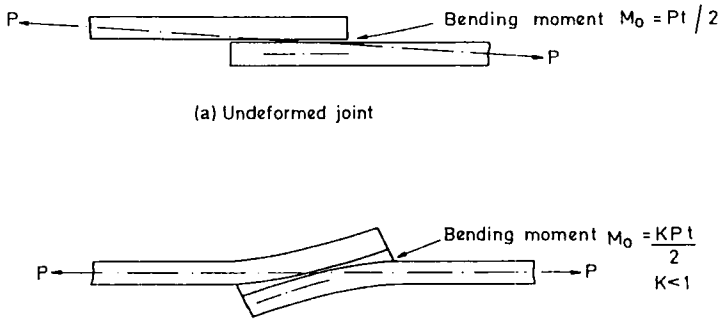

FIGURE 3 Illustrating a way of representing the Goland and Reissner bending moment factor geometrically.

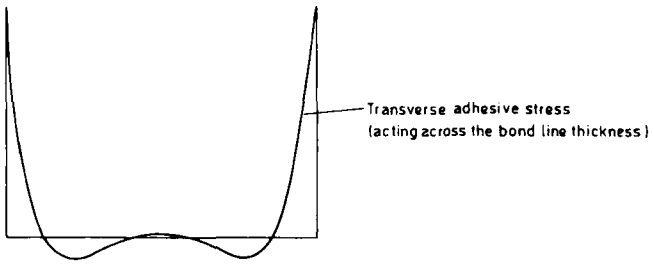

FIGURE 4 Transverse (peel) stresses in a single lap joint according to Goland and Reissner.

adhesive thickness, and it can also be seen that the maximum values of each occur at the ends of the overlap.

A double-lap joint, which is essentially two single-laps back-to-back, can be used to eliminate joint rotation because there is no net bending moment on a symmetrical double-lap joint. However, because the load is applied through the adhesive to the adherends away from their neutral axes, the double-lap joint experiences internal bending, as shown diagrammatically in Figure 5. In a symmetric double-lap joint, the centre adherend experiences no net bending moment, but the outer adherends do, thus giving rise to tensile stresses across the adhesive layer at the end of the overlap where they are not loaded, and compressive stresses at the end where they are loaded, as shown in Figure 5.

More recently, several authors, notably Renton and Vinson[4] and Allman[5] have produced analyses where the adherends have been modelled to account for bending, shear and normal stresses. They have also set the adhesive shear to zero at the overlap ends since the adhesive end has a free surface (on which the shear and direct stress must be zero) and so, by the law of complementary shears, the adhesive shear stress must also be zero at the joint ends. In addition, Allman has allowed for a linear variation of the peel stress across the adhesive thickness, although his adhesive shear stress remains constant through the thickness.

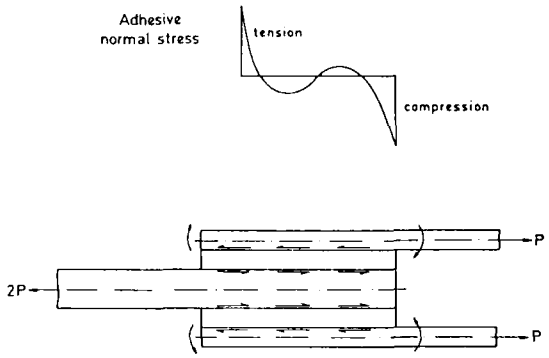

FIGURE 5 Bending moments induced in the outer adherends of a double lap joint, together with adhesive peel stresses.

By considering the three-dimensional stresses, Adams and Peppiatt[6] showed the existence of shear stresses in the adhesive layer and direct stresses in the adherends acting at right-angles to the direction of the applied load (that is, across the width of the joint), these stresses being caused by Poisson's ratio strains in the adherends. They allowed for adherend shear strains because, for many practical joints, Goland and Reissner's criteria for neglecting adherend shear strains are not applicable. This is particularly so with composite materials such as carbon fibre reinforced plastics (CFRP) because of the low in-plane shear modulus, G_{12}.

Perhaps the major conclusion from all the closed-form analyses, whether they be simple or complex, is that the maximum adhesive stresses always occur near the end of the bond line.

The main contradiction with these theories is that they all predict that the stresses will decrease as the bondline thickness increases: this is not the case in practice since bondline thickness only weakly affects lap joint strength.[7]

In algebraic lap joint analyses discussed so far, it has been assumed that the adhesive layer ends in a square edge as shown in Figure 6a. But even a rectangular plate with shear loading on its two opposite sides experiences high tensile and compressive stresses at its corners. These transverse direct stresses, similar to Goland and Reissner's peel stresses, arise because the direct and shear stresses acting on the free surface must be zero. Thus, in an adhesive layer with a square edge, similar tensile and compressive stresses must occur in the corners of

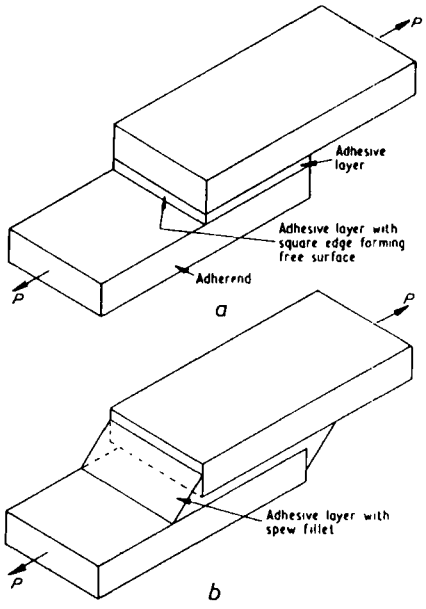

FIGURE 6 Diagrammatic lap joints to show adhesive layers with:
(a) square edge;
(b) spew fillet.

this layer because of the free surface. But practical adhesive joints rarely have a square edge: instead, they are formed with a fillet (see Figure 6b) which is squeezed out under pressure while the joint is being manufactured. Photoelastic stress analysis[8] has shown that the position of the maximum stress depends on the edge shape. Classical mathematical solutions predict that the highest stresses should be near the ends of the joint, but are unable to take into account the influence of the fillet on these stresses. But it is in just these regions of maximum stress, where failure is bound to occur, that the assumed boundary conditions of the algebraic theories are least representative of reality. Some alternative solution must, therefore, be found.

3 FINITE ELEMENT METHODS (ELASTIC CASE)

The finite element (F.E.) method is now a well-established means for mathematically modelling stress (and many other) problems. Its advantage lies in the fact that the stresses in a body of almost any geometrical shape under load can be determined. The method is, there, capable of being used for analysing an adhesive joint with a spew fillet. Figure 7 shows the principal stress pattern obtained by the finite element analysis applied to a silicone rubber model joint.[7] The length and direction of the lines represent the magnitude and direction of the principal stresses at the centroid of each element. A bar at the end of the line implies a compresive (negative) principal stress. The presence of the fillet clearly causes the stress pattern to significantly from the pattern at the end with no fillet. At the points A1 and A2, high tensile and compressive stresses are shown, while the rubber away from the ends of the steel plates is in pure shear, as is shown by the equal and opposite principal stresses in the elements in this region. The stresses in the fillet are predominantly tensile, with a maximum stress concentration at this end being at the sharp corner B.

Figure 8 shows the stress pattern at the end of a square-edged adhesive layer in a typical aluminium/aluminium lap joint bonded with a structural epoxy adhesive. The highest tensile stress exists at the corner of the adhesive adjacent to the loaded adherend and represents a stress concentration of at least 10 times the average applied shear stress.

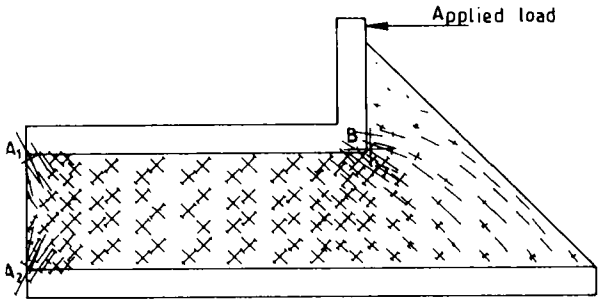

FIGURE 7 Principal stress pattern for silicone rubber model showing end effects.

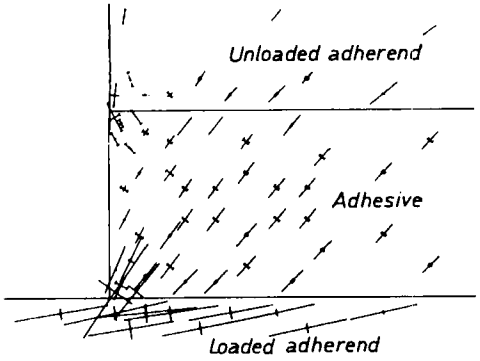

FIGURE 8 Finite element prediction of the principal stress pattern at the end of a square-edged adhesive layer.

The influence of a fillet on the stress pattern is shown in Figure 9, which is at the tension end of a double lap joint. Even though only a very small triangular fillet, 0.55 mm high, was used, the stress system is very different from that of Figure 8. Also, it can be seen that the adhesive at the ends of the adhesive layer and in the spew fillet is essentially subjected to a tensile load at about 45° to the axis of loading. The highest stresses occur near the corner of the unloaded adherend because the 90° corner introduces a stress-concentrating effect. As the maximum stress occurs within the fillet and not at or near the adhesive surface, it is unlikely that the approximation to the spew shape by the triangular fillet has a significant effect on the stress distribution.

Observation of the failure of aliminium to aluminium lap joints bonded with typical structural adhesives shows the cracks are formed approximately at

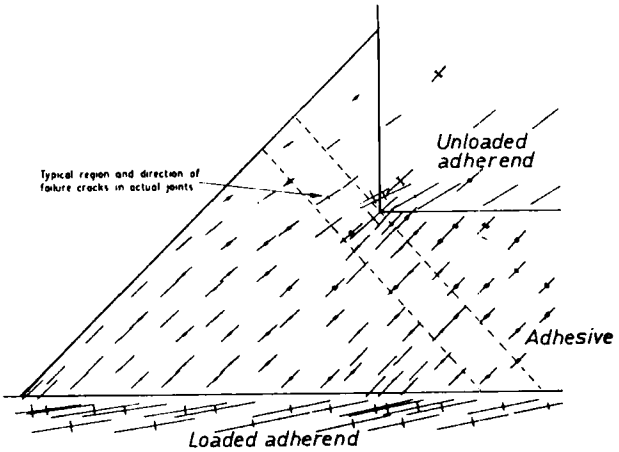

FIGURE 9 Finite element prediction of the principal stress pattern at the end of an adhesive layer with 0.5 mm spew fillet.

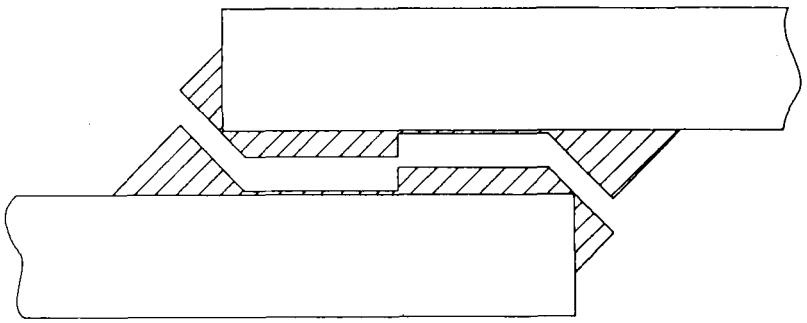

FIGURE 10 Diagram of failure surfaces of a single lap joint.

right-angles to the directions of the maximum principal stresses predicted by the elastic finite-element analysis. In general, these cracks run close to the corners of the adherends as shown in Figure 9. Thus, it can be proposed that failure in a lap joint is initiated by the high tensile stresses in the adhesive at the ends of the joint. Cohesive failure of the adhesive occurs in this manner in normal, well-bonded joints. Under further loading, the initial crack in the fillet is turned to run along (or close to) the adhesive-adherend interface. It meets a similar crack running in the opposite direction and we have the familiar fracture path shown schematically in Figure 10.

Crocombe and Adams[9] used a more advanced system of finite elements than Adams and Peppiatt,[6] choosing plane-strain, two-dimensional, rectangular, quadratic, iso-parametric elements. Figure 11 shows how the adhesive principal, peel and shear stresses vary across the adhesive thickness at different distances from the overlap end. Except within a few adhesive thicknesses from the end, the stresses are essentially uniform (as shown in Figure 7). The maximum values of

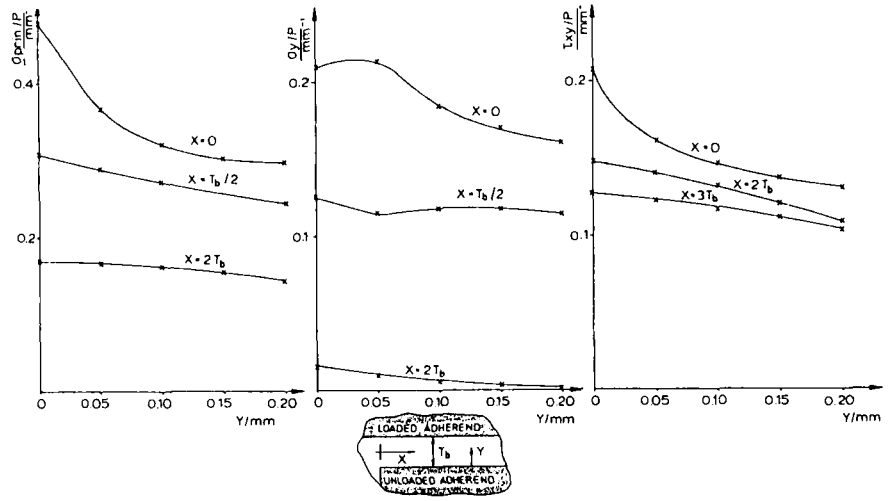

FIGURE 11 Variation of adhesive principal (σ_{prin}) and (σ_y) and shear (τ_{xy}) stresses across the adhesive thickness (y) at various distances (x) from the overlap ends.

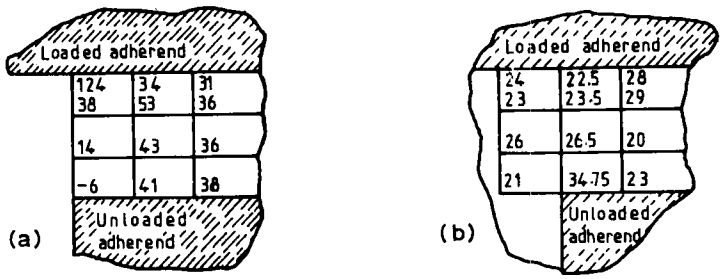

FIGURE 12 Finite-element prediction of principal adhesive stresses around the end of the overlap for:
(a) square-edged point;
(b) joint with full depth spew fillet, carrying the same load (arbitrary units).

the adhesive stresses generally occur under the overlap, the maximum principal stress being at the unloaded adherend corner, acting at about 45° to the longitudinal axis of the joint, confirming the earlier results of Adams and Peppiatt.[6] The maximum peel stress is at the overlap end, just within the adhesive layer, and the maximum shear stress is on the adhesive-adherend interface at a small distance from the overlap end.

Figure 12 shows the values of the principal stresses predicted for a square-ended adhesive layer and one with a full-depth spew fillet. It can be seen that a high tensile principal stress is predicted at the loaded adherend surface in Figure 12a and a small compressive stress at the corner. Averaging these stresses gives 59 units. Any failure criterion based on average stresses with square-ended layers would therefore be in error by about 100%. It is also in the wrong direction as far as safety is concerned. For the same joint geometry but with a full depth spew fillet (as shown in Figure 12b) the large stress gradient has almost disappeared and the average principal stress is only 28.6 units. A similar calculation with a smaller fillet (one-third full height) gave an average of 40.75 units (35.25 and 46.25 at the corner). The increase in stress was due in part to the reduced load-carrying capacity of the smaller spew fillet, but the important point is that, even in this latter case, the maximum value of the principal stress is only 37.3% of that predicted for the square ended layer, and its position has shifted across the bond-line to the corner of the unloaded adherend.

4 ELASTO-PLASTIC ANALYSIS (ALGEBRAIC AND FINITE ELEMENT APPROACHES)

Complicated mathematics is required if the stress situation in a single lap joint is to be determined algebraically. Even so, the analyses discussed so far have assumed that the adhesive and the adherends are linearly elastic. However, modern structural adhesives can develop a large plastic strain to failure. Thus, it is necessary to consider what happens to the stress distribution when the adhesive can yield. Further, these new adhesives are so strong that the adherends too may

be caused to yield. Even with the old, brittle adhesives, the adherends in single lap joints often yielded plastically in bending before the joint failed. Two opposite effects occur when the adherends yield. Increased differential straining of the adherends causes the adhesive stresses to be increased, thus leading to premature failure. However, if the adherends are stressed to yield, they will more easily rotate under the effect of the non-collinear applied loads. This causes the Goland and Reissner joint factor "k" to decrease more than if the adherends remained elastic, thus reducing the stresses. It is, therefore, necessary to investigate both adhesive plasticity and adherend plasticity, using either continuum mechanics of numerical (finite element) techniques.

Using the continuum mechanics approach, Hart-Smith[10] says that failure occurs when the adhesive reaches its limiting shear strain. When non-linear material properties are treated by a closed form analysis such as Hart-Smith's the limitation is how tractable is a realistic mathematical model of the stress-strain curve within an algebraic solution. With the finite element techniques developed for adhesive joints by the author and his co-workers, the limit becomes that of computing power. The high elastic stress and strain gradients at the ends of the adhesive layer need to be accommodated by using several 8-node quadrilateral elements across the thickness. It is then necessary to define yield (of the adhesive usually but it can also be the adherend) and then to adopt a suitable failure criterion.

Double-lap joints in which two epoxy adhesives of different strengths and strains (but still of low ductility) to failure were used, were analysed by Adams, Coppendale and Peppiatt.[11] Now the yield behaviour of many polymers, including epoxy resins, is dependent on both the hydrostatic (dilatational) and shear (deviatoric) stress components. Thus, there is a difference between the yield stresses in uniaxial tension and compression. For epoxy resins, ratios of compressive to tensile yield stresses of the order of 1.3 have been obtained by various authors. Tests on bulk specimens of two fairly brittle epoxy adhesives, (MY750 and AY103 by Ciba-Geigy) gave ratios of 1.27 and 1.14 respectively. This behaviour was incorporated into the analysis by assuming a paraboloidal yield criterion of the form

$$(\sigma_1 - \sigma_2)^2 + (\sigma_2 - \sigma_3)^2 + (\sigma_3 - \sigma_1)^2 + 2(Y_C - Y_T)(\sigma_1 + \sigma_2 + \sigma_3) = 2Y_C Y_T$$

where σ_1, σ_2 and σ_3 are a combination of principal stresses causing yield and Y_C and Y_T are the absolute values of the uniaxial compressive and tensile yield stresses. This type of yield criterion applies to many amorphous polymers over a wide range of stress states. It should be noted that when $Y_C = Y_T$ the paraboloidal yield criterion reduces to the more familiar von Mises cylindrical criterion.

Figure 13 shows the predicted variation of joint strengths with overlap length of double lap joints assuming a strain at failure of 5% for AY103 and 3% for MY750. Note that the relative tensile strengths were 71 MPa for AY103 and 85 MPa for MY750. The experimental failure loads from the double lap joint tests are also shown for comparison. The shape of the curves is similar to those obtained using the linear elastic analysis in that the predicted strength increases

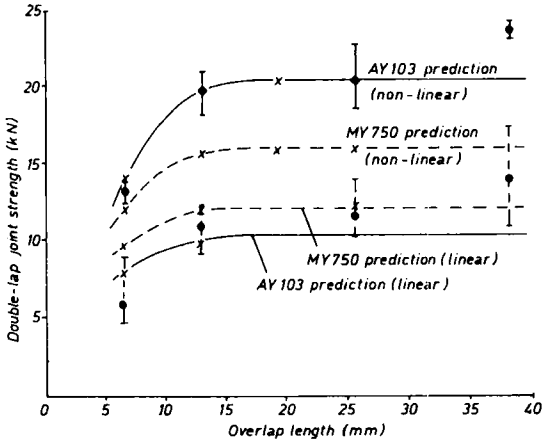

FIGURE 13 Comparison of experimental and predicted double lap joint strengths. Theoretical predictions for —x—AY103,---x---for MY750. Experimental results with error bars ⊥●⊥ AY103, ⊥●⊥ MY750.

with overlap length up to about 15 mm and then remains constant. However, unlike the linear elastic analysis, allowing for the material non-linearity has predicted the AY103 joints to be stronger than the MY750 joints, which is in broad agreement with the test results.

Figure 14 shows the relationship between the applied load and the maximum principal strain predicted at the adherend corner, for the two adhesives. At a maximum strain of 3%, the AY103 joint is supporting less load than the MY750 with a similar strain. However, if the AY103 is able to withstand a 5% strain before failure, the load carrying capacity of the joint is 27% higher than that of

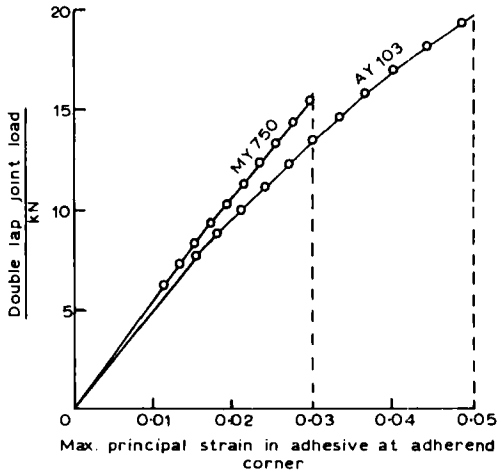

FIGURE 14 Double-lap joint load *versus* maximum principal strain in adhesive; 12.7 mm overlap; 0.13 mm adhesive thickness.

the MY750 joint at a 3% strain. This is despite the fact that the tensile strength of AY103 at a strain of 5% is less than the tensile strength of MY750 at a strain of 3%. Note that although these adhesives have some plasticity, they are still brittle by comparison with most metals.

Finite element methods for lap joints allowing for rotation of the adherends (large displacement analysis), and significant plastic deformation of both the adherends as well as the adhesive, were developed by Harris and Adams.[12] Predicted and measured joint strengths agreed well for a range of adhesives and adherends. The variation of adhesive maximum principal stresses with distance along the overlap are shown in Figure 15 for a case in which the adherend properties correspond to a relatively low strength aluminium alloy (a 0.2% proof stress of 110 MPa) and the adhesive is linearly elastic. Note that to simplify comparisons the stresses have been normalized by dividing by the average shear stress.

Under the action of tension and bending, the adherends begin to yield at an applied load of approximately 1.5 kN. At 3 kN, the adherend plastic deformation has had two effects on the adhesive stresses. Firstly, it has led to a reduction in the peak stress concentration at the end of the overlap, at point A, over and above that for the elastic case as a result of the enhancement of the joint rotation. Secondly, the concentration of adhesive stress at the ends of the fillet, point B, has increased, owing to the yield in the adherend adjacent to this point producing a localized increase in the differential shear effect. At an applied load of 6 kN,

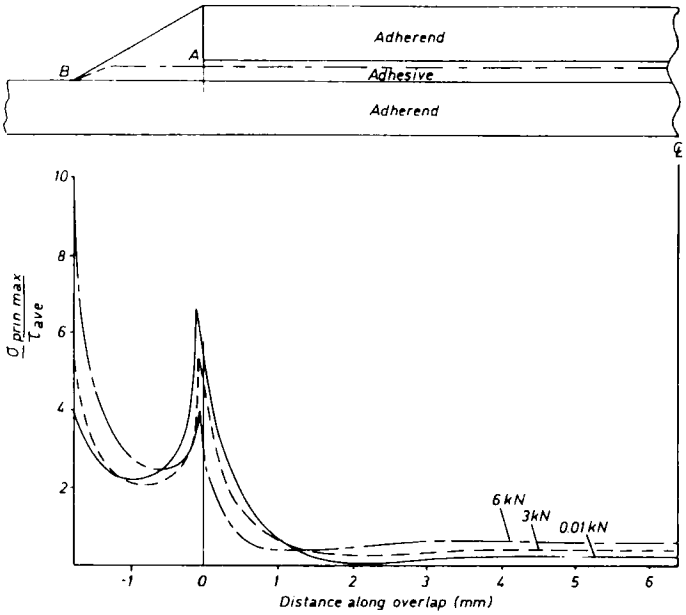

FIGURE 15 Normalized maximum principal stress distributions along the adhesive layer with adherend yielding, at various applied loads (elastic adhesive).

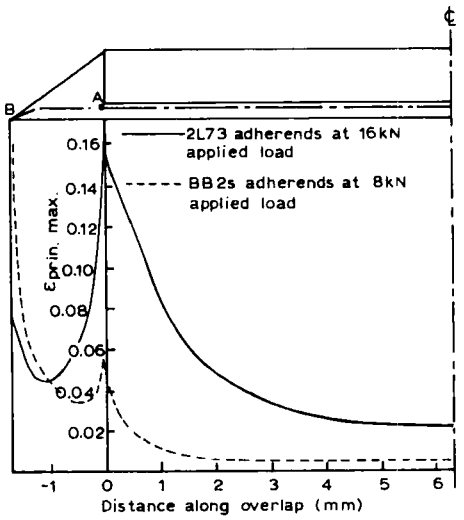

FIGURE 16 Effect of adherend yielding on the maximum principal adhesive strain distribution along the overlap for CTBN-modified epoxy. ——2L73 adherends at 16 kN applied load; - - - - -BB2s adherends at 8 kN applied load.

further plastic deformation in the adherends has taken place, leading to a dramatic increase in the peak at B, such that the stresses at this point are now the highest in the adhesive. It may be concluded, therefore, that when adherend plastic deformation takes place, the joint strength will be reduced and, at the same time, failure will no longer initiate from point A, but from point B.

The other extreme of behaviour is when a high-strength, low-ductility adherend is combined with a ductile adhesive. Figure 16 shows the computed principal strains in a CTBN (carboxyl-terminated butadiene-acrylonitrile) toughened epoxy adhesive between two 2L73 high-strength aluminium adherends. This combination gave a joint strength of 16 kN, but when ductile (low yield strength) adherends were used with the same adhesive, the joint strength was reduced by a half to 8 kN. There is a complete range of adhesive behaviour between the two extremes given here, where the failure criterion may not be based on a single parameter, such as maximum principal stress or strain. Further investigation is required into failure criteria for adhesives in order that the limits to the strength of simple lap joints, as well as more complex bonded structures, may be determined under a variety of loads. It has been found that failure in ductile adhesives best correlates with the tensile strain to failure in a bulk specimen, while in brittle adhesives (less than 3% strain to failure), tensile stress gives the best correlation. While adhesives in a single lap joint appear to be loaded in shear, they do not fail in shear. It is strongly contended that few, if any, structural adhesives fail in shear but that they fail in tension when the principal stresses or strains reach some limiting value.

5 LOCAL STRESS CONCENTRATIONS AT DISCONTINUITIES

Stress concentrations are very important in all structures, especially those joined by adhesive bonding. A sharp corner or crack causes, in theory, an infinite stress (or strain) concentration, often referred to mathematically as a singularity. Since it is impossible in reality to have an infinite stress concentration, the science of fracture mechanics has grown up to explain why such infinite stresses and strains do not exist or, alternatively, if they do exist, then why structures do not collapse under very light loads. *The fracture mechanics approach, especially with ductile adhesives in thin bond lines, must therefore be seen as intellectually suspect.* Indeed, although fracture mechanics has been used by some authors in adhesive bond studies, there is little or no evidence of a joint having been designed on this basis.

In practice, the sharp corners at the ends of a lap joint are always rounded slightly during manufacture, such as by abrasion, or by etching during surface treatment. Also, the adhesive is not linearly elastic to failure, but can yield. Finally, the author has observed experimentally that, despite the theoretical stress concentration at the corner of the unloaded adherend, the crack leading to failure rarely, if ever, cuts across the corner, but is usually about the same distance as the glue line thickness (say 0.2 mm) away from it. This implies that whatever condition it is that causes failure, it is not at the actual corner but some distance from it. The influence of the geometry of the corners in adhesive joints has been studied by Adams and Harris.[13] They showed that rounding the corner removed the singularity and produced a uniform stress field in this region, owing to the restraining effect of the relatively rigid adherend. When plastic energy density in the adhesive was analysed, it was shown that the maximum value was generally away from the corner, thus explaining why failure initiated away from the corner and not at it. Figure 17 shows results for a rigid corner with various degrees of rounding. The value of the parameter k in Figure 17 is of the same order as the effective radius at the corner, and it should be noted that 0.01 mm is about as small a radius that can reasonably be created.

Using their mathematical model, Adams and Harris were able to predict the strengths of various aluminium/aluminium joints, bonded with a rubber-toughened epoxy, and these are compared with their experimental results in Table I, where it can be seen that excellent agreement has been obtained.

6 COMPOSITE MATERIALS

One of the major advantages of adhesive bonding is that it enables dissimilar materials to be joined and so allows fibre reinforced plastics, consisting of highly aligned layers of carbon or glass fibres, to be bonded to metals. Some composites are woven or stitched so that the fibres are not perfectly alighed. High-quality chemical plant may be made from satin-weave glass fibre reinforced polyester or epoxy resin, while lower grade composites usually consist of random glass fibres in a polyester resin. Composites can be highly anisotropic in respect of both

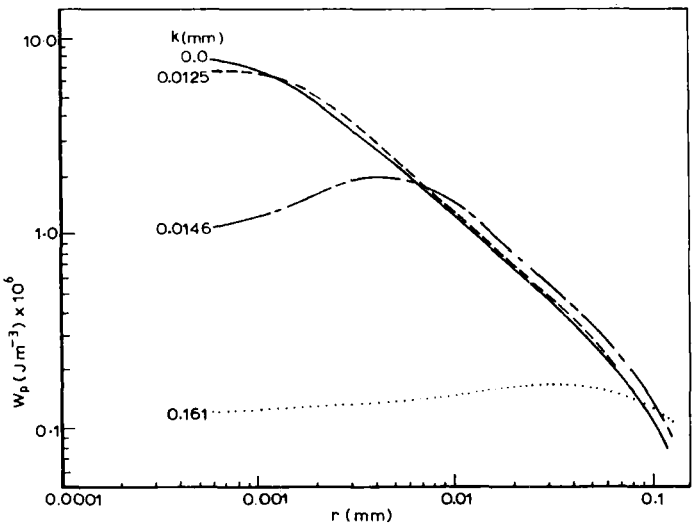

FIGURE 17 Variation of the adhesive plastic energy density distribution with corner rounding along the joint centre-line for elastic-plastic adhesive properties.

TABLE I
Comparison of joint strength predictions with experimental values

Joint type	Predicted (kN)	Experimental (median)(kN)
Square edged	14.5	15.9
Filletted	21.2	20.4
Filleted and radiused	25.3	24.5

stiffness and strength and, although a uni-directional composite may be very strong and stiff in the fibre direction, its transverse and shear properties may be weak. Bolts and rivets can sometimes be used with composites, but it is then often necessary to have load-spreading inserts *bonded* into the structure. Adhesive bonding is attractive since it allows for a more gentle diffusion of the load into the structure, thus reducing the localized stresses encountered in the use of bolts and rivets.

The techniques of analysis are essentially the same as when isotropic adherends are used, although due attention must be paid to the low longitudinal shear stiffness of unidirectional composites. The use of lamination techniques, in which fibres are placed at different angles to the plate axis, leads to reduced longitudinal and increased shear moduli. However, the *transverse* modulus (*i.e.* through the thickness of the adherend) remains low, being only two or three times that of the matrix material (usually epoxy or polyester resin). In addition, the transverse *strength* is low, usually being of the same order or less than that of the matrix. Table II lists some typical properties for carbon fibre reinforced plastics. If the joint experiences transverse (peel) loading, there is a strong likelihood that the

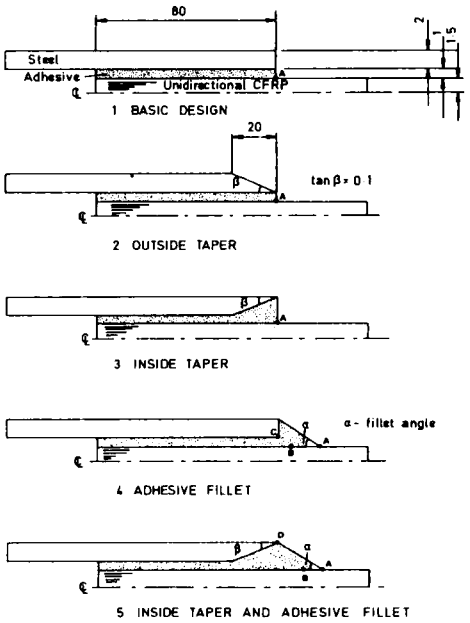

FIGURE 18 Various double lap joint designs for steel-CFRP bonding.

composite will fail in transverse tension before the adhesive fails. Adhesive peel stresses should therefore be minimized where composite adherends are used lest this leads to adherend failure.

Adams *et al.*[14] considered the stress and strain distribution in a series of joints in which CFRP was bonded to steel in the form of a double lap joint, the CFRP being the central adherend. The dimensions and various designs analysed are shown in Figure 18. Most of the designs shown in Figure 18 are modifications of the basic design, keeping the same overlap but aimed at improving joint strength. In designs 2 and 3, the outer adherends were modified by tapering; this reduces the maximum adhesive shear stress in a joint, but only if the taper is continued to a fine edge. Design 4 shows the original joint modified to include an adhesive fillet at the end likely to fail; fillets have been shown by Crocombe and Adams[9] to

TABLE II
Mechanical properties of CERP adherends

Longitudinal Young's modulus (E_1)	135	GPa
Transverse Young's modulus (E_2)	7	GPa
Interlaminar (longitudinal) shear modulus (G_{12})	4.5	GPa
Longitudinal tensile strength (σ_1)	1550	MPa
Transverse tensile strength (σ_2)	50	MPa
Interlaminar shear strength (τ_{12})	110	MPa
Longitudinal Poisson's ratio (ν_{12})	0.3	
Transverse Poisson's ratio (ν_{23})	0.3	

reduce the peak maximum principal adhesive stress. Finally, in design 5 both a taper and fillet have been incorporated.

A toughened epoxy adhesive (Ciba-Geigy XD911) was used in the experimental programme. Mechanical properties measured in a bulk adhesive specimen showed a Young's modulus of 3.05 GPa, a failure stress of 84 MPa, and a failure strain of 4.6 per cent when tested in uniaxial tension. These values were used, together with the CFRP properties given in Table II, in the computer programs for predicting the stresses, strains and failure loads of the double lap joint specimens.

Almost invariably, the most highly stressed region in an adhesive joint occurs at or near one corner. If the corner is sharp then, in theory, there exists a singularity which implies infinite stresses and/or strains at this corner. In designs 1–3 the points designated as "A" in Figure 18 are singularities, as are points "C" and "D" in designs 4 and 5. Some might argue that it should be possible to apply a fracture mechanics analysis to the singularities in these critical regions. However, the author doubts if this is reasonable and knows of no successful fracture mechanics method in which the strength of bonded lap joints has been predicted. An alternative approach can be used in which a small degree of local rounding is introduced into the finite element model in the crtical region, thus removing the singularity. In this way, the problems of dealing with singularities are avoided and failure criteria applied to the maximum conditions occurring within the predicted stress field may be employed. In practice, the corner geometries are unlikely to be perfectly square anyway, so that the modified geometries are much more likely to be realistic.

Both the steel and CFRP adherends were modelled as linearly elastic materials while, for the adhesive, yield and plastic deformation were taken into account. In addition, the finite element analysis allowed for large displacements and geometrical nonlinearity. The yield criterion for the adhesive is a function of the hydrostatic as well as the deviatoric stress component and can be derived from the form given in section 4 to give

$$[J_1(S-1)+(J_1(S-1)^2+12J_2S)^{1/2}]/2S = Y_T$$

where J_1 and J_2 are the first and second stress invariants respectively and

$$S = Y_C/Y_T$$

where Y_C and Y_T are the yield stresses in uniaxial compression and tension respectively.

For all of the joint designs considered, the peak transverse stresses in the composite occurred in the region adjacent to the edges of the outer steel adherends. These peak stress values for each joint under a load of 1 MNm^{-1} width are given in Table III. In designs 1–3, tapering the outer (steel) adherends has negligible effect on reducing the transverse direct stress, σ_T. A contour plot of the transverse stresses was produced for the critical region of design 1 (Figure

TABLE III
Predictions of the maximum transverse stresses in the CFRP from elastic finite element analysis with a 1 MN m^{-1} applied load

Design	Fillet angle	σ_T in CFRP (MPA)
1	—	38
2	—	37
3	—	36.5
4	45°	16
4	30°	10
4	17°	10
5	45°	13
5	30°	6.5
5	17°	5

19). Here, as with designs 2 and 3, a large stress concentration exists adjacent to the very edge of the adhesive layer. The abrupt edge of the adhesive layer causes the transfer of the load from the inner CFRP adherend to the outer steel adherends to be focused in this local edge region; the transverse stresses in the CFRP decay rapidly away from this location towards the centre-line of the joint

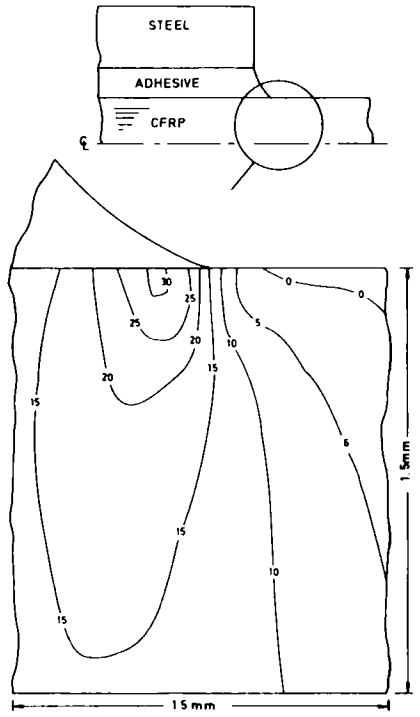

FIGURE 19 Joint Design 1; transverse stresses (MPa) in the CFRP, for an applied joint load of 1 MN/m.

and longitudinally away from the overlap. This pattern of load transfer and stress concentration is affected very little by either the outside or inside taper of designs 2 and 3. It is worth noting that prediction of the magnitude of the concentration of the transverse stress would be very difficult by closed form analytical methods, so that resorting to the use of finite elements appears justifiable.

By introducing an adhesive fillet in Design 4, an appreciable reduction is obtained in σ_T. Even the relatively small modification of a 45° fillet reduces the stress by a factor of two. The fillet reduces the focus for the transfer of load at the edge of the overlap, giving a more even distribution of the transverse stress. Figure 20 shows the stress distribution in the CFRP for a full depth 30° fillet. In comparison with design 1, the stress concentration at the corner has been avoided and the stress variation through the thickness of the CFRP is now small. A fillet angle of just under 35° reduces the maximum transverse stress in the CFRP to only one-third of that of the basic design. The angle of the fillet also influences the position at which the maximum stress occurs. For fillet angles less than 35°, σ_T is roughly at point B in Figure 18; this is inside the adhesive but approximately 0.5 mm outside the overlap. The position of B is relatively insensitive to the fillet

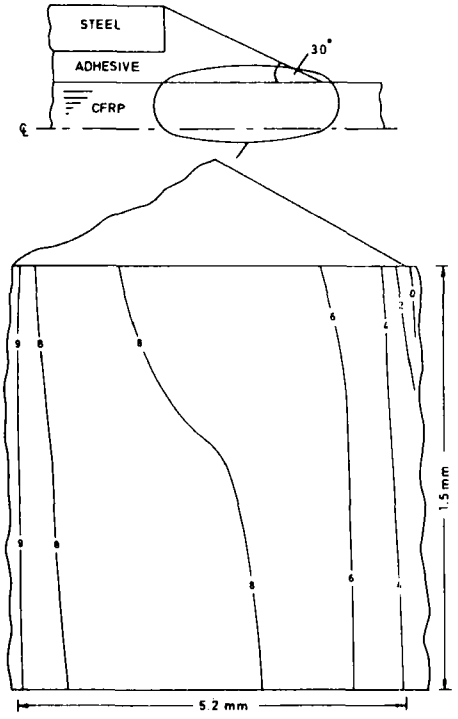

FIGURE 20 Joint Design 4 ($\alpha = 30°$): transverse stresses (MPa) in the CFRP, for an applied joint load of 1 MN/m.

angle since, for fillet angles less than 35°, the value and location of the maximum stress varies little.

A combination of an (internally) tapered steel adherend with an adhesive fillet results in further reductions in the transverse stress concentration (Design 5). In effect, the transverse stiffness is reduced at the edge of the overlap and, with the addition of an adhesive fillet, the σ_T stresses are now reduced to about a sixth of those in Design 1, so that if failure is going to occur by transverse fracture of the composite, Design 5, which includes an internal taper and an external fillet, ought to be six times stronger.

The finite element analyses also give the values of the stress components within the adhesive. From these values, the principal stresses (and hence strains) can be determined in both magnitude and direction. Cohesive failure of the adhesive occurs in regions of maximum stress or strain concentration and results in cracks which run at right angles to the direction of these (stress or strain) maxima. The principal stress distributions therefore indicate the likely locations and directions of failure in the adhesive. Not only can the joint strength then be predicted, but the fracture surfaces can be interpreted.

In Design 1 (shown in Figure 21), the highest adhesive principal stress is near to the interface with the central CFRP adherend. The direction of the stress is such that any crack initiating in this region will run towards the interface. In the case of Design 4, failure is expected to initiate near the corner of the outer steel adherend. The resulting crack will propagate both through the fillet to the free surface and in the other direction to the interface with the CFRP. With the internally tapered steel adherend, removing the corner relieves the stress concentration so that the maximum tensile stress occurs near the free surface of the adhesive fillet and adjacent to the outer steel adherend corner. Again, cracks

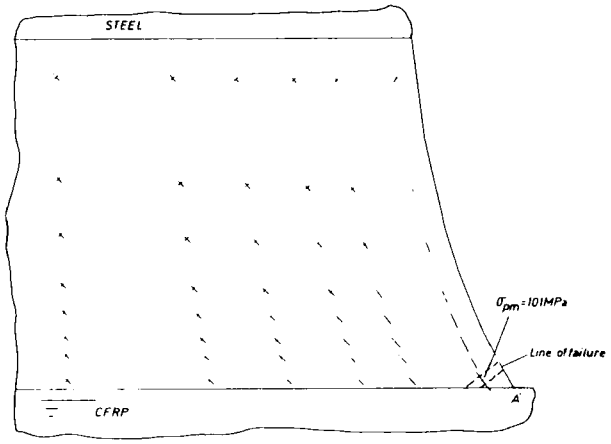

FIGURE 21 Joint Design 1: principal stress distribution, σ_p, in the adhesive at the edge of the overlap, for an applied joint load of 1 MN/m.

initiated in this region would be expected to propagate through the fillet to the interface with the CFRP as indicated.

In the experimental programme, there was no evidence of joint failure by any form of shear process. Instead, all the joints appeared to fail by interlaminar fracture of the CFRP inner adherend. Since failure was instantaneous, it was impossible to say whether it was initiated in the adhesive or in the composite. The finite element results indicated that initiation was probably in the composite for Designs 1, 2 and 3, and in the adhesive for the others. In the latter case, the crack would penetrate the adherend and result in eventual interlaminar failure. The predicted strength and modes of failure are given in Table IV, where the lower load predicted theoretically is that which should be responsible for failure. Bearing in mind the approximations made in the mathematical modelling and the variations in experimental conditions, the agreement between the lowest theoretical failure load and the actual experimental failure load was good. Although not directly covered in the theoretical treatment, it is worth reporting some additional tests carried out on single lap joints. In these joints, aluminium or steel adherends were bonded to unidirectional CFRP. Three series of specimens were used which corresponded to Designs 1, 4 and 5 in Figure 18. The experimental results, averaged for both types of adherend, each with two different fillet angles, are summarized in Table V.

The results in Table V show enormous differences between the three cases, even though the overlap areas were identical. For the double lap joints, the improvement between Designs 1 and 5 was only 3.07. This was because the double lap configuration tends to reduce the bending effects present in the single lap joint, whereas for the single lap joints the improvement was 5.35 times.

TABLE IV
Comparison of experimental joint strengths (per unit width) with theoretical predictions

Joint Design					
No	Description	Fillet angle	Experimental failure load (MN/m)	Interlaminar CFRP failure* (MN/m)	Tensile adhesive failure* (MN/m)
1	Basic	90°	0.93	1.05‡	1.6
2	Outside taper	90°	0.89	1.08‡	—
3	Inside taper	90°	0.94	1.10‡	—
4	Adhesive fillet	45°	—	2.7‡	—
4	Adhesive fillet	30°	—	4.24‡	2.0
4	Adhesive fillet	17°	—	4.24‡	—
5	Inside taper† Adhesive fillet	45°	2.72	3.53	4.0
5	Inside taper† Adhesive fillet	30°	3.05	7.44	3.3
5	Inside taper† Adhesive fillet	17°	2.80	9.08	2.4

* Based upon a maximum transverse, interlaminar strength of 40 MPa.
† Based upon a maximum principal (tensile) strain of 0.0475.
‡ From elastic analysis (otherwise elastic-plastic analysis).

TABLE V
Single lap joint stengths for steel or aluminium bonded to CFRP

Joint design (*cf.* Figure 18)	Description	Failure load	Ratio
1	Basic	4.85	1
4	Basic + fillet	9.53	1.96
5	Inside taper + fillet	25.93	5.35

7 CONCLUDING REMARKS

Analytical techniques such as those of Volkersen, Goland and Reissner, and others cannot be used to predict the strength of adhesively-bonded lap joints without using some form of uncertainty factor. This is simpy because their analytical equations cannot adequately describe the real stress and strain conditions at the ends of the joint where failure is bound to occur.

Finite element techniques can accommodate non-linear mechanics (joint rotation), non-linear material properties, adhesive fillets, and corner rounding. It has been shown that the finite element technique can be successfully used for predicting the strength of lap joints.

In the case of joints with composite adherends, there are two possible mechanisms of failure. In one case, transverse tensile stresses at the edge of the joint close to the interface result in interlaminar failure of the CFRP. In the other case, concentrations of the principal stresses in the adhesive result in tensile (cohesive) failure. The cohesive failure results in cracks which run through the adhesive to the interface, after which the composite will fail transversely in an interlaminar manner. However, it may not be clear in the first instance which mechanism is responsible for failure from studying only the fractured surfaces of the joint. By applying suitable failure criteria to the finite element results for the adhesive and the adherends, the load required for failure by either mechanism can be predicted. Interlaminar failure in the composite used here was calculated by using a maximum tensile transverse stress of 40 MPa. Cohesive failure of the adhesive was predicted by using a maximum principal tensile strain (4.75%) of a bulk sample of the adhesive in uniaxial tension, which is very similar to the state of stress in the critical regions of the adhesive.

Thus, by using finite element techniques, it is possible to predict the strength of joints from fundamentals together with the node of failure. This greatly assists not only the design process but also the post-failure analysis of joints, as it otherwise is difficult, if not impossible, to decide where the failure initiated.

References

1. R. D. Adams, W. C. Wake, *Structural Adhesive Joints in Engineering*" (Applied Sci. Publs., London & New York, 1984).
2. O. Volkersen, *Luftfahrtforschung* **15,** 41–47 (1938).
3. M. Goland, E. Reissner, *J. Appl. Mechanics: Trans. Am. Socy. Mech. Engineers* **A66,** 17–27 (1944).

4. W. J. Renton, J. R. Vinson, *J. Adhesion* **7,** 175–193 (1975).
5. D. J. Allman, *Quart. J. Mechanics & Appl. Math.* **30,** 414–436 (1977).
6. R. D. Adams, N. A. Peppiatt, *J. Strain Anal.* **8,** 134–139 (1973).
7. R. D. Adams, N. A. Peppiatt, *J. Strain Anal.* **9,** 185–196 (1974).
8. C. Mylonas, *Proc. Socy. Experimental Stress Anal.* **12,** 129 (1954).
9. A. D. Crocombe, R. D. Adams, *J. Adhesion* **13,** 141–155 (1981).
10. L. J. Hart-Smith, in *Developments in Adhesives 2,* A. J. Kinloch, Ed. (Appl. Science Publs., London, 1981), p. 1.
11. R. D. Adams, J. Coppendale, N. A. Peppiatt, in *Adhesion 2,* K. W. Allen, Ed. (Appl. Sci. Publs., London, 1978), p. 105–119.
12. J. A. Harris, R. D. Adams, *Intern. J. Adhesion & Adhesives* **4,** 65–78 (1984).
13. R. D. Adams, J. A. Harris, *Intern. J. Adhesion & Adhesives* **7,** 69–80 (1987).
14. R. D. Adams, R. W. Atkins, J. A. Harris, A. J. Kinloch, *J. Adhesion* **20,** 29–53 (1986).